Electron-phonon coupling origin of the graphene π^*-band kink via isotope effect

F. Bisti [1,2,*] A. V. Fedorov [3,4] M. Donarelli [1] M. Fantasia [1] L. Petaccia [5] O. Frank [6] M. Kalbac [6]
G. Profeta [1,7] A. Grüneis [8] and L. Ottaviano [1,7]

[1]*Dipartimento di Scienze Fisiche e Chimiche, Università dell'Aquila, Via Vetoio 10, 67100 L'Aquila, Italy*
[2]*ALBA Synchrotron Light Source, 08290 Cerdanyola del Vallès, Spain*
[3]*IFW Dresden, Leibniz Institute for Solid State and Materials Research, D-01171 Dresden, Germany*
[4]*Helmholtz-Zentrum Berlin für Materialien und Energie, 14109 Berlin, Germany*
[5]*Elettra Sincrotrone Trieste, Strada Statale 14 km 163.5, 34149 Trieste, Italy*
[6]*J. Heyrovský Institute of Physical Chemistry, Czech Academy of Sciences, Dolejškova 3, CZ-18223 Prague 8, Czech Republic*
[7]*CNR-SPIN L'Aquila, Via Vetoio 10, 67100 L'Aquila, Italy*
[8]*II Institute of Physics, University of Cologne, Zülpicher Strasse 77, 50937 Cologne, Germany*

The π^*-band renormalization of Li-doped quasifreestanding graphene has been investigated by means of isotope (^{13}C) substitution and angle-resolved photoemission spectroscopy. The well documented sudden slope change (known as "kink") located at 169 meV from the Fermi level in the graphene made of ^{12}C atoms shifts to 162 meV once the carbon monolayer is composed by ^{13}C isotope. Such an energy shift is in excellent agreement with the expected softening of the phonon energy distribution due to the isotope substitution and provides, therefore, an indisputable experimental proof of the electron-phonon coupling origin of this well known many-body feature in the electronic structure of graphene.

I. INTRODUCTION

Many-body interactions within charge carriers are of great interest in condensed matter physics due to their capability of destabilizing conventional metallic states leading them to new exotic ground states. Among them, the most notable example is the intimate connection of the electron-phonon coupling (EPC) with superconductivity. In angle-resolved photoemission spectroscopy (ARPES) such interactions are detected as strong renormalization or abrupt changes (typically referred to as "kinks") of the band dispersion in the proximity of the Fermi level. Being not reproducible in a single electron band theory, these sudden deviations are then generically ascribed to many-body effects. The ARPES investigation of kinks has been fundamental for the study of high-T_c cuprate superconductors [1,2]. To this end, an interesting strategy has been the isotopic substitution of oxygen, offering a controlled investigation of the presence of EPC (or lack thereof): For the nodal kink, the observation of few meV energy shift in agreement with the isotopic shift of phonon frequency has been used to directly demonstrate its EPC nature [3].

In graphene, the coupling within quasiparticles has been extensively investigated and the kink at around 169 meV below the Fermi energy in a strongly doped scenario has been generally attributed to EPC [4–9]. The plausibility of this assignment is justified by a likely coupling between the conduction electrons and the E_{2g} and A'_1 in-plane optical phonons [5,10], since both the Eliashberg function and the

phonons density of states of the system present peaks around the energies of E_{2g} and A'_1 [7,11]. This assignment is of high interest because of the suggested theoretical strategy of inducing a superconducting phase through the classical phonon mediated process where EPC is the pairing mechanism [12]. A very recent theoretical study has shown that dopant adatoms could give an important contribution to the quasiparticle band renormalization, with a possible abrupt change in the same energy region of the observed kink in the graphene π^* band [13]. In this scenario, the adatom-induced kink might be obscuring the EPC contribution. Spin fluctuation has been recently suggested to be the mechanism behind the strong renormalization of the band in the proximity of the van Hove singularity [14]. Even though the theoretical calculations were not suggesting abrupt changes [14] in the band renormalization, this possibility cannot be completely excluded. Moreover, the origin of superconductivity in twisted bilayer graphene [15] is still debated and theoretically interpreted either within a nonconventional [15,16] or within a conventional electron-phonon origin [17]. The possibility of a clear experimental demonstration of an electron-phonon coupling for the electrons at the Fermi energy by means of ARPES experiments [18] would give important hints along this line. However, measurements of ARPES isotope effect in graphene is challenging and needs still to be demonstrated.

In graphene, isotope substitution is experimentally viable with ^{13}C. More marked isotopic substitutions are impossible due to the ^{14}C instability. "Heavy" graphene (^{13}C) has been already successfully grown via chemical vapor deposition using methane as precursor gas, and the expected softening of graphene phonons by the $\sqrt{12/13}$ (about 0.96) factor has been detected in the Raman spectra [19,20]. To the best of

*fbisti@cells.es
†fabio.priante@aalto.fi

our knowledge, the isotope substitution method in ARPES has been only applied to the cuprates family, with the only exception of a single work on MgB_2 [21], and never attempted so far on two-dimensional systems. In this context, such investigation on graphene has the potential not only to determine the kink origin, but also to represent a solid textbook example in the field due to the extreme simplicity of the graphene band structure.

Here, we report an experimental ARPES study of the π^*-band dispersion renormalization of Li-decorated graphene in the proximity of the Fermi level by adopting the approach of ^{12}C-^{13}C isotope substitution. By the comparison of the spectra features between "normal" (^{12}C) and "heavy" graphene we discriminate the EPC contribution from other possible electron interactions, like adatoms scattering or spin fluctuation. We propose a particularly robust data analysis methodology that entails four different routes, with three of them completely free from any assumption on the noninteracting quasiparticle band dispersion. Noteworthy, independently on the different data treatments, we report an energy shift of the kink (of 6–9 meV), consistent with the expected phonon softening. This unequivocally proofs the EPC as the main contribution of the kink at 169 meV from the Fermi level and gives a strong and direct experimental validation on the related EPC studies based on this ARPES feature [4–9].

II. METHODS

Pristine monolayer graphene samples were prepared [7,11] *in situ* under ultrahigh vacuum conditions by chemical vapor deposition on Ni(111) thin films epitaxially grown on W(110), using ethanol ("normal" or "heavy" with 99 atom% ^{13}C from Sigma-Aldrich) as carbon precursor. Low-energy electron diffraction (LEED) was performed on the Ni(111) films to monitor the film crystallinity. To decouple graphene from the Ni substrate (making it quasifreestanding) one monolayer of Au was subsequently deposited and intercalated into the graphene/Ni interface by annealing [22,23]. Lithium was then stepwise evaporated from commercial SAES metal dispensers and home-built evaporators. ARPES data were collected at the BaDElPh beamline of the Elettra Synchrotron (Trieste, Italy) [24] using 29 eV photon energy, with *p* polarization (*s* polarization) for scanning along the KM (ΓK) direction of the graphene Brillouin zone. The sample temperature was kept below 30 K. The total energy and angular resolutions were set to 20 meV (full-width-at-half-maximum of the Gaussian model fitting the experimental Fermi edge) and 0.1°, respectively. To check for reproducibility and improve results robustness, the experiment was repeated on three different samples for both ^{12}C graphene and ^{13}C graphene. After ARPES investigation, one sample each of "normal" and "heavy" graphene were quality checked (*ex situ*) via micro-Raman spectroscopy with a system operating in ambient conditions (LabRAM HR spectrometer, Horiba Jobin-Yvon, equipped with an Olympus BX microscope, using 600 lines/mm grating for dispersing the scattered light yielding 1.8 cm^{-1} point-to-point spectral resolution). The Raman spectrometer was calibrated before each set of measurements at the F_{1g} line of Si at 520.2 cm^{-1}. The spectra
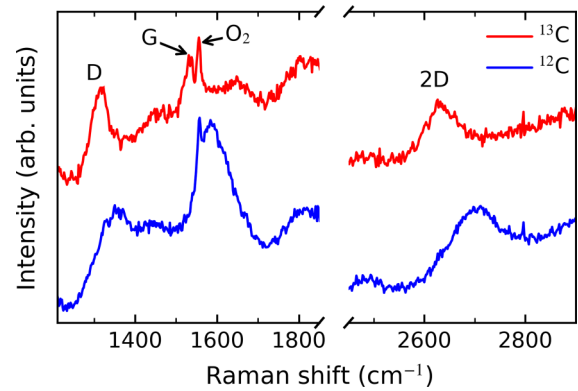
FIG. 1. Comparison of the Raman spectra of D, G, and 2D peaks for ^{12}C (blue) and ^{13}C (red) graphene. On the left (right) side of the G peak for ^{12}C (^{13}C) graphene there is the oxygen peak (O_2) from the ambient air.

were acquired using a 488 nm excitation wavelength of an Ar^+/Kr^+ laser source with 0.75 mW power under a 100× microscope objective. Because of the air exposure during the Raman investigation, the graphene samples were not doped with lithium.

III. RESULTS AND DISCUSSION

In Fig. 1, we report the Raman spectra for ^{12}C and ^{13}C samples: A shift towards lower energies of a ∼0.96 factor is observed for the G, D, and 2D peaks of the ^{13}C samples, confirming a successful and complete isotopic substitution [20]. In Fig. 2, we report the ARPES overview of the Dirac cone for the different samples (top panels). From the Fermi surface area extension we estimate an effecting electron doping of about 2×10^{14} cm^2, corresponding to a shift of -1.4 eV of the Dirac point due to Li deposition, for all the investigated cases. In the top panels of Fig. 2, we show how the ΓK branch of the Dirac cone is well reproduced by a single-electron nearest-neighbors tight-binding model of the graphene band structure (using the parameters of $\gamma_0 = -2.848$ eV, $s_0 = 0.0029$, and $\epsilon_{2p} = 0.1$ eV as in Ref. [25]). On the contrary, we find a strong band renormalization along the KM direction, which has been recently interpreted as originating from electronic correlations due to spin fluctuations [14]. The slight changes in the band dispersions for the three different samples with the same carbon isotope, instead, reflect the variability of the lithium deposition: Different amounts and arrangement of the adatoms on the sample give different electric fields and charge doping with slight modifications of the Dirac cone position and the band structure dispersion [8]. Such effects on the band structure, which are intrinsic to the doping procedure, are superimposed on the kink structure in proximity of the Fermi level at around 169 meV on both branches of the Dirac cone.

This observation opens a delicate discussion on how to disentangle the extrinsic effects due to the dopant from the intrinsic presence of the kink in the measured band dispersion. The origin of the kink is due to many-body interactions affecting the band dispersion with an additional complex *k*- and energy(ω)-dependent self-energy, $\Sigma(k, \omega)$, contribution
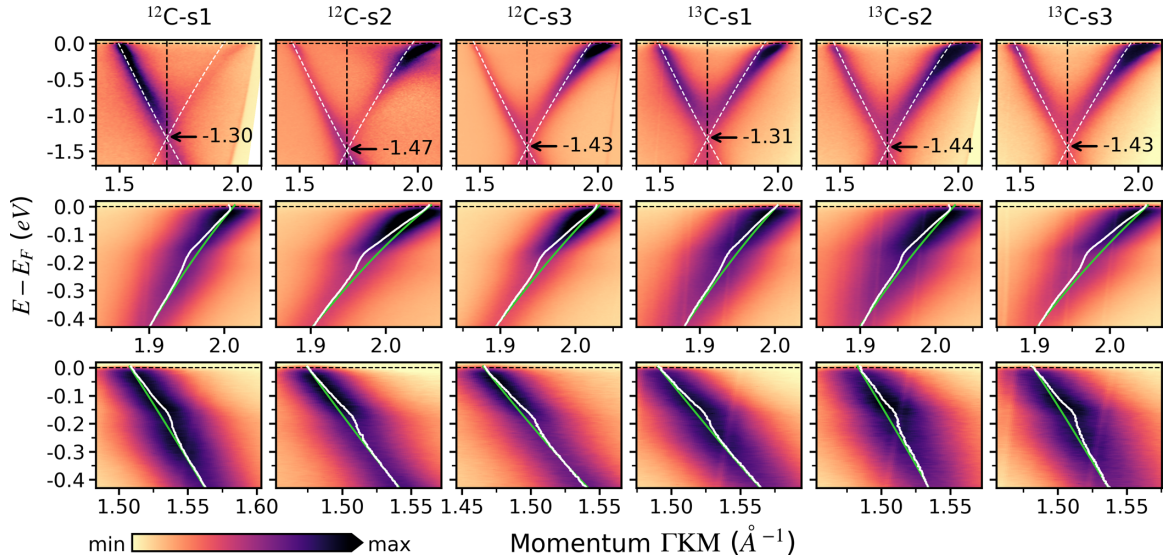
FIG. 2. Dirac cone dispersions along the ΓKM direction. On top panels, the data are a linear combination of the *s*- and *p*-polarization signals for Dirac cone enhancing purposes (with the exception of the ^{12}C-s1 sample where only *s* polarization is reported). Arrows point to the binding energy position of the Dirac cone. Dashed white lines on top panels are first-nearest-neighbor tight-binding calculated electronic structures rigidly shifted in energy to match the different doping levels. On middle (bottom) panels, the high resolution ARPES spectra are plotted along KM (ΓK) directions with the extracted band dispersion from MDC analysis (white lines) and the bare bands resulting from the self-consistent analysis (green lines).

to the noninteracting band (bare band). Although a convenient and more realistic choice for the bare band, used to reveal the kink position, could be obtained from first-principles density functional theory (DFT), the presence of the alkaline disorder would prevent a direct comparison with the experiment even introducing artificial contributions because of the periodicities of the models [26,27]. Moreover, additional dopant renormalization effects would not be still reproduced in a single-electron picture [14]. Thus, the only viable solution is in practice an experimental determination of the bare band.

The detailed analysis of the band dispersion is reported in Fig. 2, where high resolution ARPES spectra are overlaid with the extracted band dispersions (white lines) and the related bare bands (green lines). The experimental band dispersions were obtained from momentum dispersion curves (MDCs) analysis, as the center (k_m) of fitted asymmetric Lorentzian shapes [28] with a linear background. The bare bands were modelled using third order polynomials whose coefficients were calculated by a self-consistent procedure: Minimizing the differences between the extracted ReΣ and the Hilbert transformation ($\mathcal{H}$) of extracted ImΣ [9], since the two quantities are intertwined via Kramers-Kronig relations (see Supplemental Material for the self-consistent derivation of the bare band for each sample [29]). The real and imaginary part of the self-energy are then obtained as $\text{Re}\Sigma(\omega) = (k_m - k_m^b)v^b(\omega)$ and $\text{Im}\Sigma(\omega) = -\delta k_m v^b(\omega)$, where k_m^b and $v^b(\omega)$ are the bare band momentum and band velocity at energy ω, respectively, while δk_m is the half width at half maximum.

The resulting ReΣ and ImΣ for the various samples are shown in Figs. 3(a) and 3(b), along KM and ΓK directions. The kink position for each curve (represented by red and blue thick marks, for ^{12}C and ^{13}C samples, respectively) are determined by the maxima of ReΣ convoluted with a

Gaussian line shape on Fig. 3(a). The average peak position [represented by the black dashed lines in Fig. 3(a)] is found at 169 meV for the ^{12}C graphene and 161–162 meV for the ^{13}C graphene. The ReΣ(ω) essentially peaks at the E_{2g} phonon frequency [5,30], thus the observed 7–8 meV shift between ^{12}C and ^{13}C samples is then due to the change in the E_{2g} phonon frequency caused by isotope substitution. The expected isotope softening of graphene phonons for complete ^{12}C/^{13}C substitution is of $\sqrt{12/13}$ (about 0.96) factor, which implies a reduction from 169 meV to 162 meV with a shift of 7 meV, in excellent agreement with the experimental result. From the repetition of the same experiment on the same graphene type we were also able to extract a reproducibility error of ± 2 meV (± 3 meV) in the determination of the kink energy position along the KM (ΓK) direction. So, despite the experimental broadening of the Fermi level, our data analysis drastically reduces the indetermination on the kink energy position.

As already explained, the method applied so far for the kink analysis implies a careful determination of the bare band. In the following we validate our results via three other alternative methods for the kink analysis (as in Ref. [31]), having the peculiarity of not requiring any bare band pre-knowledge. These procedures are based on the analysis of $\frac{d^2}{d\omega^2}k(\omega)$, of $\mathcal{H}(\frac{d}{d\omega}k(\omega))$ and $\frac{d}{d\omega}\delta k(\omega)$, where $k(\omega)$ and $\delta k(\omega)$ are the k_m and δk_m, respectively, obtained from the MDC analysis filtered by the convolution with a Gaussian shape. Practically, one method is a second derivative analysis giving an estimation of the k_m curvature, and, in the case of a linear bare band, it is directly proportional to the second derivative of the ReΣ [31]. The second and the third one can be considered as the coupling strength distribution as a function of the quasiparticle energy [31]. Despite not giving quantitatively
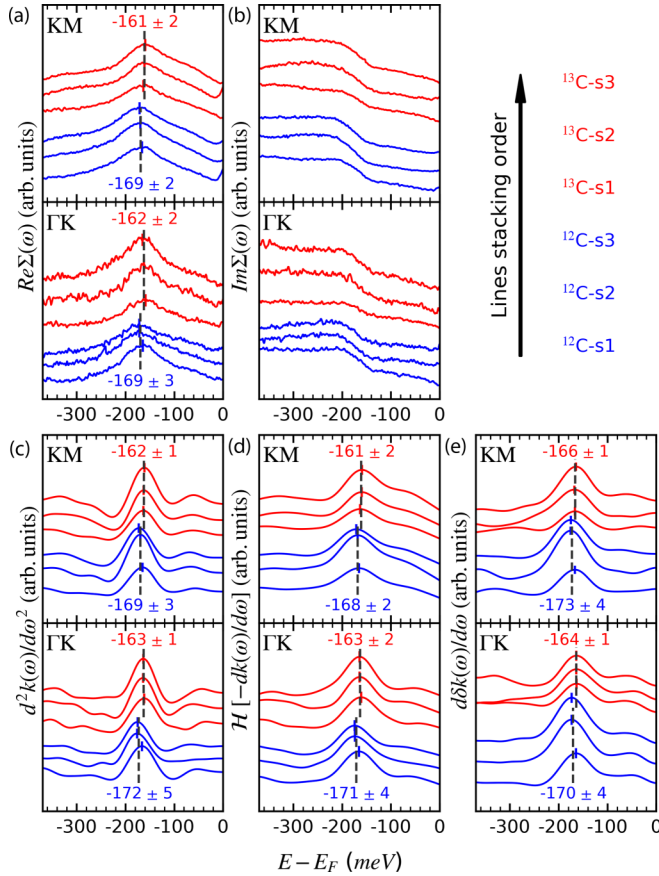
FIG. 3. (a) Comparison between ^{12}C (blue) and the ^{13}C (red) graphene samples of the ReΣ (a), ImΣ (b), the second derivative (c), and Hilbert transform of the first derivative (d) of $k(\omega)$ obtained from MDCs, and the first derivative (e) of $\delta k(\omega)$ obtained from MDCs. In panels (c), (d), (e), the y axis is reversed in ΓK with respect to KM for clarity.

the Re$\Sigma(\omega)$, these methods are nevertheless efficient in determining the number and energy position of the kinks. The results obtained by these alternative three methodologies are reported in Figs. 3(c) and 3(d): The main peaks can be identified in almost the same positions of our main analysis, with an observed shift of the kink position of 6–9 meV between ^{12}C and ^{13}C graphene. This further strengthens our proof of the occurrence of the EPC isotopic shift, as its derivation is free from any choice on the bare band and in direct connection with only the k_m and δk_m, as obtained from the MDC analysis.

In Fig. 3(c), an additional kink seems to emerge at a binding energy of about 60 meV, mostly visible along the KM direction. A similar low-energy kink was reported in literature and assigned to the electrons coupled with alkaline dopant vibrations [8]. Being only present along KM we cannot exclude this renormalization to be also a manifestation of the

recently theorized Li-induced charged-impurity scattering, instead of being located at the energy of the main peak [13]. The energy region is also compatible with graphene-related acoustic phonons, but since the reproducibility error (± 3 meV) is comparable to a carbon phonon isotopic shift occurring at this energy scale (~ 3 meV), the ^{12}C-^{13}C comparison cannot be used in this case to support or exclude any assignment. Finally, in the Supplemental Material [29] we report a detailed analysis on the EPC strength (λ): As expected from theory (see equation S1) its variation is determined only by the different doping level of the samples rather than their carbon mass.

IV. CONCLUSIONS

In conclusion, via ARPES and isotopic substitution (^{12}C with ^{13}C) we have monitored the many-body self-energy interactions in the π^*-band renormalization of Li-decorated graphene, directly detecting a kink energy shift from 169 meV to 162 meV, in excellent agreement with the expected softening of the phonon energy. This demonstrates, at the same time, (i) the achieved experimental accuracy to measure the isotope shift, (ii) the assessment of a robust analysis framework for data analysis, (iii) the proof of EPC origin of the kink observed in ARPES experiments, thus excluding other possibilities, as for example adatoms scattering or spin fluctuations, and (iv) definitively supports previous ARPES investigations on such band renormalization of graphene based on the EPC hypothesis. The present demonstration of the carbon isotope substitution effectiveness on the kink analysis can promote possible extension in other graphene systems, as twisted bilayer graphene [15] or strongly doped scenarios [9,32–34], but also for the understanding of superconductivity in related carbon-based materials (graphite intercalation compounds [35], carbon nanotubes [36], C$_{60}$ [37,38]) for which graphene constitutes a useful model system. Finally, we believe that, given the simplicity of the graphene band structure, this study itself represents a perfect textbook example for ARPES investigation of the isotopic substitution effects and band renormalization.

[1] A. Damascelli, Z. Hussain, and Z.-X. Shen, Rev. Mod. Phys. **75**, 473 (2003).

[2] T. Cuk, D. H. Lu, X. J. Zhou, Z.-X. Shen, T. P. Devereaux, and N. Nagaosa, Phys. Status Solidi (b) **242**, 11 (2005).

[3] H. Iwasawa, J. F. Douglas, K. Sato, T. Masui, Y. Yoshida, Z. Sun, H. Eisaki, H. Bando, A. Ino, M. Arita, K. Shimada, H. Namatame, M. Taniguchi, S. Tajima, S. Uchida, T. Saitoh, D. S. Dessau, and Y. Aiura, Phys. Rev. Lett. **101**, 157005 (2008).

[4] A. Bostwick, T. Ohta, T. Seyller, K. Horn, and E. Rotenberg, Nat. Phys. **3**, 36 (2007).

[5] M. Calandra and F. Mauri, Phys. Rev. B **76**, 205411 (2007).

[6] D. A. Siegel, C.-H. Park, C. Hwang, J. Deslippe, A. V. Fedorov, S. G. Louie, and A. Lanzara, Proc. Natl. Acad. Sci. **108**, 11365 (2011).

[7] D. Haberer, L. Petaccia, A. V. Fedorov, C. S. Praveen, S. Fabris, S. Piccinin, O. Vilkov, D. V. Vyalikh, A. Preobrajenski, N. I. Verbitskiy, H. Shiozawa, J. Fink, M. Knupfer, B. Büchner, and A. Grüneis, Phys. Rev. B **88**, 081401(R) (2013).

[8] A. V. Fedorov, N. I. Verbitskiy, D. Haberer, C. Struzzi, L. Petaccia, D. Usachov, O. Y. Vilkov, D. V. Vyalikh, J. Fink, M. Knupfer, B. Büchner, and A. Grüneis, Nat. Commun. **5**, 3257 (2014).

[9] B. M. Ludbrook, G. Levy, P. Nigge, M. Zonno, M. Schneider, D. J. Dvorak, C. N. Veenstra, S. Zhdanovich, D. Wong, P. Dosanjh, C. Straßer, A. Stöhr, S. Forti, C. R. Ast, U. Starke, and A. Damascelli, Proc. Natl. Acad. Sci. **112**, 11795 (2015).

[10] A. Politano, F. de Juan, G. Chiarello, and H. A. Fertig, Phys. Rev. Lett. **115**, 075504 (2015).

[11] A. Grüneis, C. Attaccalite, A. Rubio, D. V. Vyalikh, S. L. Molodtsov, J. Fink, R. Follath, W. Eberhardt, B. Büchner, and T. Pichler, Phys. Rev. B **80**, 075431 (2009).

[12] G. Profeta, M. Calandra, and F. Mauri, Nat. Phys. **8**, 131 (2012).

[13] K. Kaasbjerg and A. P. Jauho, Phys. Rev. B **100**, 241405(R) (2019).

[14] S. Link, S. Forti, A. Stöhr, K. Küster, M. Rösner, D. Hirschmeier, C. Chen, J. Avila, M. C. Asensio, A. A. Zakharov, T. O. Wehling, A. I. Lichtenstein, M. I. Katsnelson, and U. Starke, Phys. Rev. B **100**, 121407(R) (2019).

[15] Y. Cao, V. Fatemi, S. Fang, K. Watanabe, T. Taniguchi, E. Kaxiras, and P. Jarillo-Herrero, Nature (London) **556**, 43 (2018).

[16] M. Angeli, E. Tosatti, and M. Fabrizio, Phys. Rev. X **9**, 041010 (2019).

[17] B. Lian, Z. Wang, and B. A. Bernevig, Phys. Rev. Lett. **122**, 257002 (2019).

[18] I. Razado-Colambo, J. Avila, J. P. Nys, C. Chen, X. Wallart, M. C. Asensio, and D. Vignaud, Sci. Rep. **6**, 27261 (2016).

[19] X. Li, W. Cai, L. Colombo, and R. S. Ruoff, Nano Lett. **9**, 4268 (2009).

[20] O. Frank, L. Kavan, and M. Kalbac, Nanoscale **6**, 6363 (2014).

[21] D. Mou, S. Manni, V. Taufour, Y. Wu, L. Huang, S. L. Bud'ko, P. C. Canfield, and A. Kaminski, Phys. Rev. B **93**, 144504 (2016).

[22] A. Varykhalov, J. Sánchez-Barriga, A. M. Shikin, C. Biswas, E. Vescovo, A. Rybkin, D. Marchenko, and O. Rader, Phys. Rev. Lett. **101**, 157601 (2008).

[23] M. H. Kang, S. C. Jung, and J. W. Park, Phys. Rev. B **82**, 085409 (2010).

[24] L. Petaccia, P. Vilmercati, S. Gorovikov, M. Barnaba, A. Bianco, D. Cocco, C. Masciovecchio, and A. Goldoni, Nucl. Instrum. Methods Phys. Res., Sect. A **606**, 780 (2009).

[25] M. Kralj, I. Pletikosić, M. Petrović, P. Pervan, M. Milun, A. T. N'Diaye, C. Busse, T. Michely, J. Fujii, and I. Vobornik, Phys. Rev. B **84**, 075427 (2011).

[26] F. Bisti, G. Profeta, H. Vita, M. Donarelli, F. Perrozzi, P. M. Sheverdyaeva, P. Moras, K. Horn, and L. Ottaviano, Phys. Rev. B **91**, 245411 (2015).

[27] N. Ehlen, M. Hell, G. Marini, E. H. Hasdeo, R. Saito, Y. Falke, M. O. Goerbig, G. Di Santo, L. Petaccia, G. Profeta, and A. Grüneis, ACS Nano **14**, 1055 (2020).

[28] D. Y. Usachov, A. V. Fedorov, O. Y. Vilkov, I. I. Ogorodnikov, M. V. Kuznetsov, A. Grüneis, C. Laubschat, and D. V. Vyalikh, Phys. Rev. B **97**, 085132 (2018).

[29] See Supplemental Material at http://link.aps.org/supplemental/10.1103/PhysRevB.103.035119 for self-consistent derivation of the bare band for each sample and detailed analysis of the EPC strength (λ).

[30] C. H. Park, F. Giustino, M. L. Cohen, and S. G. Louie, Nano Lett. **8**, 4229 (2008).

[31] H. Anzai, M. Arita, H. Namatame, M. Taniguchi, M. Ishikado, K. Fujita, S. Ishida, S. Uchida, and A. Ino, Sci. Rep. **7**, 4830 (2017).

[32] S. Ichinokura, K. Sugawara, A. Takayama, T. Takahashi, and S. Hasegawa, ACS Nano **10**, 2761 (2016).

[33] J. Chapman, Y. Su, C. A. Howard, D. Kundys, A. N. Grigorenko, F. Guinea, A. K. Geim, I. V. Grigorieva, and R. R. Nair, Sci. Rep. **6**, 23254 (2016).

[34] A. P. Tiwari, S. Shin, E. Hwang, S.-G. Jung, T. Park, and H. Lee, J. Phys.: Condens. Matter **29**, 445701 (2017).

[35] S. L. Yang, J. A. Sobota, C. A. Howard, C. J. Pickard, M. Hashimoto, D. H. Lu, S. K. Mo, P. S. Kirchmann, and Z. X. Shen, Nat. Commun. **5**, 3493 (2014).

[36] R. Barnett, E. Demler, and E. Kaxiras, Phys. Rev. B **71**, 035429 (2005).

[37] A. P. Ramirez, Physica C: Supercond. Appl. **514**, 166 (2015).

[38] M. Mitrano, A. Cantaluppi, D. Nicoletti, S. Kaiser, A. Perucchi, S. Lupi, P. Di Pietro, D. Pontiroli, M. Riccò, S. R. Clark, D. Jaksch, and A. Cavalleri, Nature (London) **530**, 461 (2016).